The Pennsylvania State University

The Graduate School

Department of Engineering Science and Mechanics

A GENERAL STUDY OF A COLLOIDAL QUANTUM DOT LUMINESCENT SOLAR CONCENTRATOR

A Thesis in

Engineering Science

by

Jeremy J. Low

Submitted in Partial Fulfillment
of the Requirements
for the Degree of

Master of Science

December 2009

The thesis of Jeremy J. Low was reviewed and approved* by the following:

Jian Xu
Associate Professor of Engineering Science and Mechanics
Adjunct Professor of Electrical Engineering
Thesis Advisor

Matthew Fetterman
Adjunct Professor of Engineering Science and Mechanics

S. Ashok
Professor of Engineering Science and Mechanics

Patrick M. Lenahan
Distinguished Professor of Engineering Science and Mechanics

Judith Todd
Professor of Engineering Science and Mechanics
P. B. Breneman Department Head of Engineering Science and Mechanics

*Signatures are on file in the Graduate School

Abstract

A general study on a luminescent solar concentrator (LSC) was conducted. A Monte Carlo simulation based on ray tracing model was developed as a mean to get a better understanding and find the optimal values for parameters affecting the device performance. The effects of a few selected parameters were discussed and a feasibility study was conducted as well to probe the potential of implementing LSC to reduce the cost of solar electricity generation. It was discovered that a square LSC is more desirable than a rectangular LSC. Unfortunately, the LSC is still not a feasible idea using the lead selenide (PbSe) quantum dots discussed in this paper.

Table of Contents

LIST OF FIGURES

LIST OF TABLES

ACKNOWLEDGEMENTS

I would like to thank Matt Fetterman for his collaboration in the luminescent solar concentrator simulation work. I would also like to thank GoldSim Technology Group for providing a free copy of their simulation software. The work is funded by Army Research Office.

Chapter 1

Introduction

Solar energy is a very attractive energy source because it is practically unlimited. As the call for renewable energy is gaining momentum, solar power generation is getting a lot more attention. Unfortunately it is still expensive to harness the sun's power because of the cost of solar cells. One promising candidate for reducing the cost of solar power generation is the luminescent solar concentrator (LSC). Luminescence is the radiation of light induced by an energy source [1]. All luminescence described here is induced by sunlight.

The idea of using LSC as a way to reduce the cost of solar power generation first came about around mid 1970s [2-3]. LSC has a renewed interest these days because of the availability of new materials such as colloidal quantum dots, more efficient fluorescent dyes, and near-IR dyes. LSC is an optical device for concentrating sunlight into a small area of solar cells located at the edges of the LSC using fluorescent materials. LSC has the potential of drastically cutting the cost for solar electricity generation. This is done by replacing a large area of expensive solar cells in a solar panel with inexpensive materials and a very small area of solar cells at the edges. An advantage this device has over other solar concentrators is its ability to use both diffused and direct sunlight, therefore abolishing the need of expensive sun-tracking systems. Diffused light is the scattered sunlight after passing through the Earth's atmosphere [4]. Also LSC only have a very slight drop in efficiency on a cloudy day [2, 5]. This is because direct sunlight is

mostly blocked by the clouds and scattered, leaving mostly diffuse sunlight. Since the LSC is an efficient diffused light absorber, its efficiency is only affected slightly [2, 5].

A basic LSC has fluorescent materials that absorbs sunlight and directs it towards the small area of solar cells at the edges of the panel. Fluorescence is a type of luminescence where the radiation emission happens over a very short period of time [1]. The typical LSC uses organic fluorescent dyes as the fluorescent materials. The biggest advantage of this system is its lower cost than other types of LSCs and the dyes' high fluorescent quantum yield (FQY). This material system has the disadvantage of higher reabsorption loss than other LSCs because of the big overlap of the dyes' absorption and emission spectra. It also has a low lifetime because of the dyes' vulnerability to photo-bleaching. An improvement over the usual type of LSC is to use fluorescent dyes in conjunction with rare earth materials like neodymium and ytterbium [2]. This system has lower reabsorption loss, high FQY, and high stability. But the drawback of using rare earth materials is their low absorption coefficient, which leads to a need for much higher solution concentration, resulting in a higher cost [6]. Another possible material system is to use colloidal quantum dots (QDs) instead of organic fluorescent dyes. This system has low reabsorption loss because of its narrow emission spectrum. It also has a considerably higher lifetime than organic dyes. The disadvantages of this type of LSC are its low FQY and the high cost of the QDs.

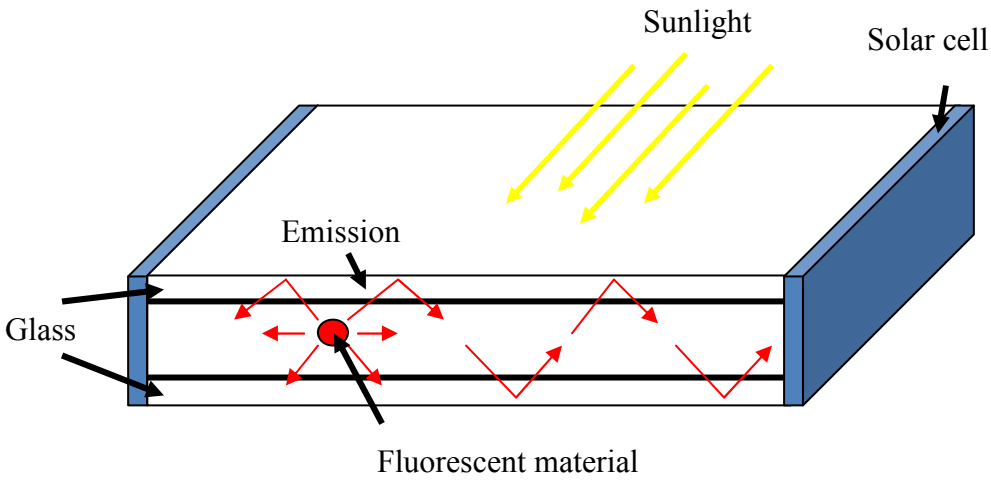

Figure 1: Basic schematic of a LSC

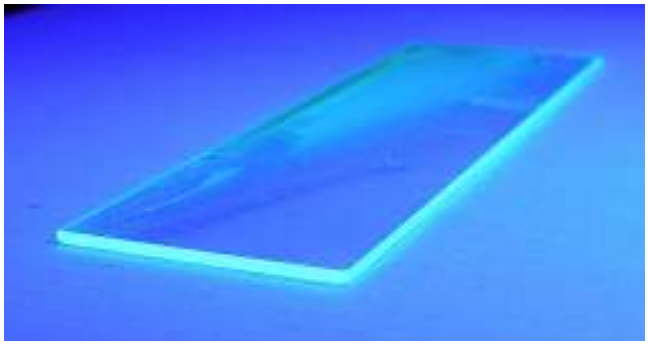

Figure 2: A LSC showing the concentrated light at the edges (color)

Chapter 2

Theory of Operation

In this chapter, the main principles and important parameters in the operation of a LSC will be covered. These include total internal reflection, loss through escape cone and reabsorption, flux gain, geometric gain, optical efficiency, and external quantum efficiency.

2.1 Absorption and emission spectrum

Absorption is the single most important parameter in a LSC. If sunlight is not absorbed, then there will not be any emission. Therefore the first parameter to consider should be the absorption spectrum of the fluorescent material(s). Next would be the emission spectrum of the fluorescent material(s). It is desirable to have a narrow emission spectrum with a large Stokes shift [7]. The Stokes shift is the shift of the emission peak from the absorption peak. Given an identical emission spectrum, a larger Stokes shift, i.e. a larger difference between the emission and absorption peak, means there is less overlap between the two spectra. Furthermore, dyes or QDs can be chosen such that their emission peaks coincide with the wavelength that maximizes the efficiency of the solar cell at the edges, or vice versa. For a solar cell with a certain band gap, the maximum efficiency occurs for incoming photons with energy slightly above that of the band gap because less energy would be wasted compared to higher energy photons.

Commercial dyes available have absorption peaks that span across the visible into the near ultraviolet and near infrared spectrum. For a single type of dye, its absorption

spectrum is limited to a small part of the solar spectrum. Dyes in general also have a broad emission spectrum, which is undesirable in a LSC. One interesting way to work around the single dye absorption spectrum limitation is to use multiple dyes. By combining three, or even four types of dyes, and using a principle called Forster Resonance Energy Transfer (FRET), absorbed energy can be transferred non-radiatively to a final emission dye [8-9].

QDs are interesting in the study of LSC because their absorption or emission peaks can be tailored through fine-tuning their sizes. QDs such as PbSe QD have a very broad absorption spectrum that span the whole visible and near infrared spectrum. They also have a much narrower emission spectrum than dyes in general, which is desirable.

2.2 Fluorescence quantum yield (FQY)

FQY is a fundamental property of a fluorescent material. It is has a value between 0 and 1, defined as the ratio of photons emitted and photons absorbed. It is the probability of emission for every photon absorbed. It is a very important parameter in a LSC because a low probability of emission will translate to lower efficiency. A high FQY means that the LSC will have high efficiency. Dyes generally have high FQY (>0.85) while QDs have relatively low FQY (~0.1 – 08). The FQY also have a slight dependence on the solvent used, which is another consideration in a LSC.

2.3 Total internal reflection

The main working principle behind LSC is total internal reflection. Whenever a ray of light strikes an interface between two mediums of different refractive indices at an oblique angle larger than a certain critical angle, it will be totally and internally reflected.

The critical angle can be determined from Snell's law, $n_1 \sin\theta_1 = n_2 \sin\theta_2$, where n_1 and n_2 are the mediums' refractive indices, and θ_1 and θ_2 are the incident angle and the refraction angle, measured relative to normal. By letting n_2=1 (for air), and θ_2=90°, the critical angle θ_c is then,

$$\theta_c = \sin^{-1}\left(\frac{1}{n_2}\right).$$

This parameter is critical in determining one of the major loss mechanisms in LSCs.

2.4 Escape cone loss

In a LSC, a waveguide must be formed within the device to confine the emitted light. Ideally, it is desirable to confine as much light as possible. The defining parameter is the critical angle. As mentioned earlier, any light emitted with an angle larger than θ_c will be reflected internally, and hence confined within the LSC. If the light emitted at an angle smaller than θ_c, then it will be lost. The escape cone is defined as the cone swept by θ_c when rotated 2π radians.

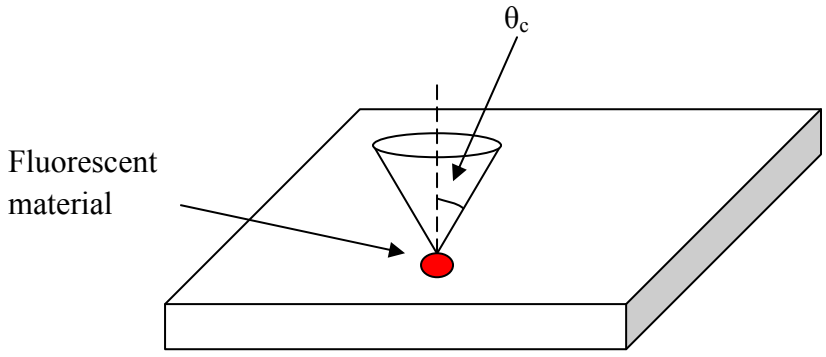

Figure 3: Escape cone

The amount of light trapped is found by looking at the ratio of the area swept outside of the escape cone to the area of a sphere.

$$A_{out} = r^2 \int_0^{2\pi} \int_0^{\pi-\theta} \sin\theta d\theta d\phi = 4\pi r^2 \cos\theta$$

Since the area of a sphere is $4\pi r^2$, the ratio is then given by $\cos\theta_c$. For glass with refractive index of 1.5, θ_c is 41.8°, and the amount of light trapped is about 74.5%. The escape cone is going to be determined ultimately by the material chosen to be on top of the LSC. It is of course desirable to have a very high refractive index material, but materials with high refractive indices (>1.8) are not available commercially. Common inexpensive materials that are used for LSC are glass, PMMA, or PET.

One possibility of combating the escape cone loss is through a hot mirror. A hot mirror is a coating on top of a LSC that permits the short wavelength light through at the front surface but reflects long wavelength light at the back surface. It was suggested that the usage of a hot mirror can provide up to 25% gain in the LSC efficiency [6]. The downside is of course the increased cost of applying such a coating.

2.5 Reabsorption loss

Whenever a photon is emitted from the luminescent material, there is a chance that it will be reabsorbed before it reaches the edge. It turns out that the reabsorption process is very significant in LSC [7, 10-12].

This reabsorption is proportional to the amount of overlap between the absorption and emission spectrum and the absorption coefficient, denoted here as α. A big overlap will ensure a high reabsorption loss, which translates to low efficiency. This is the reason a large Stokes shift (the shift in the emission peak with respect to the absorption peak) is

desirable. A parameter that is useful in looking at the reabsorption loss qualitatively is the ratio of absorption coefficient at absorption peak to the absorption coefficient at the emission peak [12]. Another factor that influences the reabsorption loss is the solution concentration. While a higher solution concentration can ensure more absorption of the incident light, it also means that the probability that an emitted photon will be reabsorbed before reaching the edge increases exponentially. Logically there should be an optimal solution concentration and this was confirmed in other literature [7].

The reabsorption loss can be quantified through the application of Beer-Lambert law,

$I = I_0 e^{-\alpha d}$, where

I_0 is the initial light intensity, α is the absorption coefficient, and d is the length the photon has to travel. The intensity can be thought of as synonymous with the number of photons, since the intensity is proportional to the number of photons. In essence, the equation can ultimately describes the number of photon reaching the collecting edges, which is important in simulation such as a ray-tracing model. The absorption coefficient can be experimentally obtained through either a transmission or absorption measurement with a spectrometer.

In general, QDs have relatively low reabsorption loss because of their narrow emission spectrum. Since the spread in QDs' emission spectrum is due mainly to the distribution in the dot sizes, better processing methods can further narrow the emission spectrum. Organic dyes, which generally have broader emission spectrum, have larger reabsorption loss.

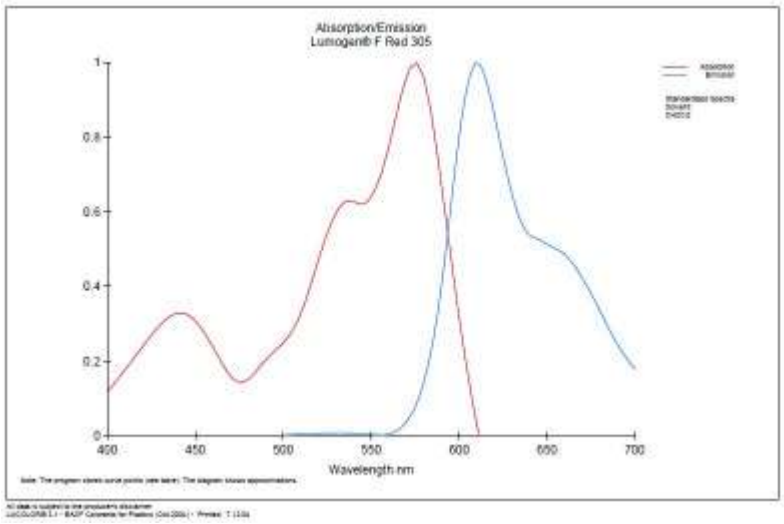

Figure 4: The emission spectrum of Lumogen F Red 305 dye, obtained from BASF.

Even when the emitted photon is reabsorbed, all is not lost because there is still a chance for it to be re-emitted again. The chance for the photon to be re-emitted has to again take into account the fluorescent material's FQY.

2.6 Mirrors

One way to enhance the efficiency of LSC is to use a mirror at the back. The purpose of the mirror is to reflect light that was not absorbed in the first pass for a second chance to be absorbed, hence increasing the absorption probability. However, since metallic mirrors such as silver mirrors are not perfect (~7% loss), there should be an air gap between the LSC and mirror [4, 13]. Even so, a loss of 7% is rather large considering that usually many passes are required before the light gets to the edge.

Instead of a mirror, a white scattering layer can be used as well [13-14]. The purpose of the white scattering layer is two-fold: to reflect the transmitted light so it can

be reabsorbed, and to redirect light that are outside of the absorption spectrum to the collecting edges. Debije [13] has shown that the addition of a white scattering layer increase the LSC output significantly, around 30 – 50%.

2.7 Optical efficiency and external quantum efficiency

The optical efficiency, η_{opt}, is defined as the fraction of photons reaching the collecting edges. It does not take into account the efficiency of the solar cell nor the coupling loss between the waveguide and solar cell at the edges. It is only a measure of the material system used. The optical efficiency is useful in comparing the performances of fluorescent materials that emit around the same wavelength. The optical efficiency is also easier to be measured than the external quantum efficiency in specific cases [7].

The external quantum efficiency, η_{EQE}, defined as the number of electron generated per photon, takes into account the solar cell efficiency and the coupling loss as well. Unfortunately this measurement is difficult to do [14]. For a theoretical calculation [11-12],

$$\eta_{EQE} = \eta_{QE}\eta_{abs}\frac{\eta_{PL}\eta_{trap}(1-r)}{1-r\eta_{PL}\eta_{trap}}, \text{ where}$$

η_{QE} is the quantum efficiency of the solar cell, η_{abs} is the absorption probability, η_{PL} is the fluorescent material's FQY, η_{trap} is the trapping efficiency, given by $\cos\theta_c$, and r is the average probability that an emitted photon will be reabsorbed. The expression for r is rather complicated, but can be simplified with a few assumptions as shown by Currie [12]. Letting the emission spectrum be a delta function and the LSC be a square, the average reabsorption probability, r, can be simplified to

$$r = 1 - \frac{2\int_{\theta_c}^{\pi/2} \sin\theta d\theta \int_{-\pi/4}^{\pi/4} d\phi \; Exp\left[\frac{-2AG\ln(10)}{\sin\theta\cos\phi}\right]}{\pi\cos\theta_c}$$, where

A is the LSC absorbance at the emission peak, given by $A = \alpha_{PL} d$, and α_{PL} is the absorption coefficient at the emission wavelength.

Noting that all the terms after η_{QE} can be summarized as the optical efficiency,

$\eta_{EQE} = \eta_{QE}\eta_{opt}$.

This expression yields a relatively easy way to calculate η_{EQE} in a simulation where the output is the optical efficiency.

2.8 Flux gain and geometric gain

The geometry of a LSC plays an important role as well. One way to quantify the geometry contribution is the geometric gain, G, defined as

$$G = \frac{\text{Total top area}}{\text{Total side area}}.$$

Naturally a high G value is desire because that would mean more cost savings. There is a limit to G, however, because as the LSC dimensions increases, so does the reabsorption loss. The next step is to find out the optimum value for G, and this is done by looking at another parameter, the flux gain, F. The flux gain is a measure of how much light is concentrated at the edge. This is the value that ultimately needs to be at its highest because it measures how well a solar concentrator concentrates light. It is defined as [11],

$F = \frac{G\eta_{conc}}{\eta_{PV}}$, where

η_{conc} is the LSC efficiency, given by $\eta_{conc} = \dfrac{\text{Output power of LSC}}{\text{Incident power}}$, and η_{PV} is the solar cell efficiency.

Assuming perfect coupling between the LSC and solar cell, the flux gain can also be defined as $F = G\eta_{opt}$. As an example, using the approximate expression of r from above the flux gain, the graph of F vs. G can be plotted [12]. Note that the graph of F vs. G is not linear because η_{conc} is a function of G as well from the calculation of the average reabsorption probability.

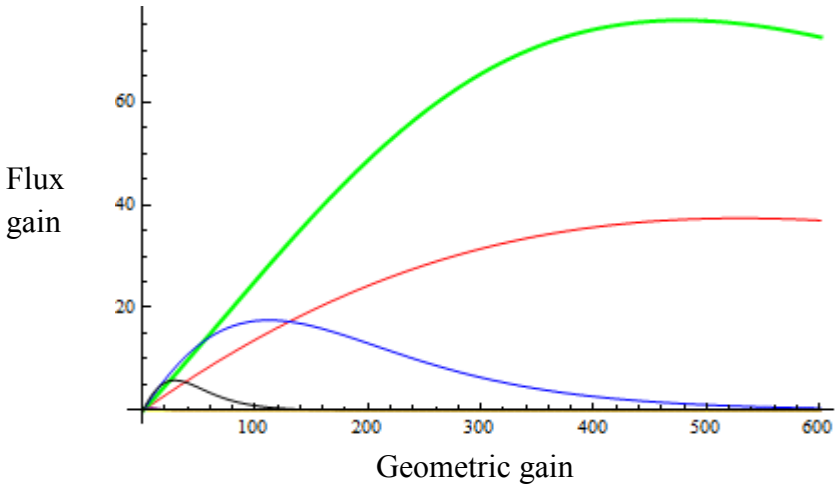

Figure 5: The graph of F vs. G showing an optimal G for different materials.

2.9 Cost per watt

If the concept of LSC is to become feasible for power generation, its cost per watt must be competitive with conventional power generation. However, since the main purpose of a LSC is to reduce the power generation cost as compared to regular solar cell,

its cost per watt must be smaller than that of the solar cell. The cost per watt can be calculated using a simplified cost model [12],

$$\left(\frac{\$}{W}\right)_{LSC} = \frac{\text{collector cost}}{\eta_{conc} P} + \frac{1}{F}\left(\frac{\$}{W}\right)_{\text{solar cell}}, \text{ where}$$

P is the power of sunlight incident on LSC.

For a LSC to be practical, F must be larger than 1.

2.10 Lifetime

Another crucial factor in the LSC implementation is the device lifetime. This is fundamentally a property of the fluorescent material because glass and polymer such as PMMA can last for a very long time. Since the device oxidation can be minimized with packaging, the next biggest factor (assuming near-perfect manufacturing conditions) for device degradation is then solar radiation, more specifically around the UV portion. Organic dyes can only last a few months under solar radiation, but with a UV-blocking coating, a stability of many years has been reported [15-16]. QD generally have better stability than organic dyes. Of particular interest is the exciting ability for QD to have a dark-cycle recovery, where 30-40% of total degradation was recovered with 12 hours of darkness [17]. This is good news because about half the day is in darkness on average.

Chapter 3

Fabrication Methods

In this chapter, different fabrication methods for the LSC will be discussed. These include the fabrication method for thin film and liquid-filled LSC.

3.1 Thin film LSC

Thin film based LSC is of particular interest because of its ease of packaging and its potential on flexible substrates. Three ways for deposition of a thin film will be discussed. Two main important properties that need to be considered are its thickness and surface uniformity. If the sample is too thin, then most light will pass right through it. If the sample surface is too rough, then the LSC performance will suffer because the thin film will not form a good waveguide. Also of importance is the host matrix material. The host matrix must be clear (to allow light to reach the fluorescent material), cheap, and does not have significant absorption in the fluorescent material working spectrum. An example of a material that satisfies those conditions is poly(methyl methacrylate) (PMMA), or more commonly known as acrylic glass.

3.1.1 Spin coating

Spin coating is popular for creating thin films on the order of 10 – 100 nm thickness because it is generally consistent in creating good quality films. It can also be done fairly quickly and easily. A spin coater works by holding the substrate in place via a vacuum and spinning the solution-covered substrate at a high rate of speed.
Spin coating is great for applications where really thin films are needed but not for LSC. For films on the order of 100 nm, the transmission is generally more than 90%. This

means that less than 10% of the incoming light will be absorbed, bringing the maximum theoretical efficiency to less than 10%. As such, spin coating is a bad candidate for creating a thin film LSC.

3.1.2 Dip coating

Dip coating is another method popular in creating thin film devices. A dip coater works by submerging the substrate in a bath of solution and slowly lifting it up through a stepper motor. Unfortunately, a thin film made by a dip coater has around the same characteristic as a spin coated film. This means that it is limited in capabilities with respect to LSC as a spin coater.

3.1.3 Spray coating

Another way to create a thin film is through spray coating. It works by spraying the target solution layer by layer onto a cleaned substrate, very much like the spray painting done in outdoor painting. Films created by this method can have a thickness on the order of microns and surprisingly smooth surfaces. Since the film thickness is about 100 thicker than that of films created by the other two methods, spray coating might be a feasible method for creating thin film LSC. The downside of this method is the user. Since the film application is not automated by a machine, irregularities of film thicknesses and quality will vary over a big range. It is speculated that it is possible to minimize this variation by automating this process. One interesting way to improve the film quality was by first spin coating a layer of thin film on the substrate before spray coating.

Figure 6: The spray coater

As a demonstration, a batch of PbSe QDs, dissolved in chlorobenzene along with PMMA was prepared. The solution concentration of the PbSe QDs is 10mg/mL, and the ratio of QD to PMMA is 1:1. Substrates were first thoroughly cleaned with soap, DI water, acetone, and isopropyl alcohol, which then went through a UV-ozone process. Samples were created by spin coating, dip coating, and spray coating for comparison. The different parameters in spray coating that can be controlled were also briefly studied.

The first sample was prepared by spin coating at 1000 rpm for 40s. The second sample was prepared with a dip coater with a pull up speed of 5 mm/min. The third sample was prepared by spray coating, at 4 psi pressure, and 80 passes. The samples' thicknesses and roughness were then measured with a profilometer.

Table 1: Comparison of coating methods

Method	Thickness (nm)	Rq (nm)
Spin coating	38.5	3.14
Dip coating	33.0	8.00
Spray coating	5858.0	3.50

Rq is a measure of the surface roughness, defined as the RMS average of surface height,

$$Rq = \left(\frac{1}{L} \int_0^L y^2 dx \right)^{1/2}$$, where

L is the sampling length, and y is the relative height of the curve of the profile.

Table 2: Variation of pressure and passes on thickness

Pressure (psi)	# of sprays	Average thickness (nm)	Rq (nm)
4	20	1075	3.65
6	20	649	5.34
10	20	311	3.22
4	10	502	3.99
4	20	1075	3.65
4	30	2158	3.02
4	40	2465	3.91

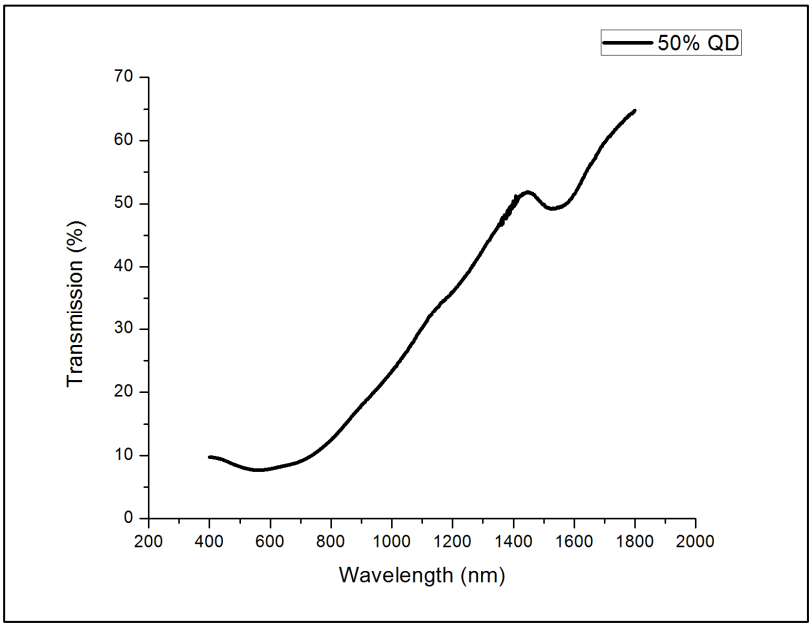

Figure 7: The transmission data for the thin film prepared from spray coating

As can be seen from Table 1, the spray coating method yields a film thickness of more than 150 times than the spin coating method, while still maintaining similar roughness. The two things that can be controlled in the spray coater was the pressure and how many layers to apply. A low pressure is desirable because the high pressure will blow the solution away from the substrate. An important determination of the roughness is the substrate condition. The substrate must be cleaned thoroughly to ensure good quality film. From an ellipsometry measurement, the film refractive index was estimated to be around 1.51. Overall the spray coating method is definitely a feasible method to prepared thin film LSC because of the ability to deposit micron-thickness films and it is fairly inexpensive.

3.2 Liquid-filled LSC

Instead of a thin film, LSC can also be prepared as a liquid-filled, or solution based LSC. This is usually done by molding glass together through optical epoxy, filling it with the sample solution, and closing the opening with optical epoxy. This is also the most common way to prepare LSC by far.

The solution LSC is also generally more efficient than thin film LSC because dyes and QDs generally have higher FQY in solution. It is also easier to make because there is no host matrix and film quality to be concerned of. For a given material, only the solution concentration and the LSC thickness play an important role in the determining the device performance.

Chapter 4

Monte Carlo Simulation Based on Ray Tracing Model

A simulation program can be invaluable in the work of LSC because it allows for tweaking of different parameters with ease to their optimal values. There are already two main methods that were developed to handle LSC simulation. The first one is a thermodynamic model and the second is a ray tracing model.

A QD based simulation was already developed by Gallagher [18]. She simulated large quantities (> 1 billion) of individual QDs in her model. This can lead to a computationally exhaustive procedure. Sholin [7] and Burgers [19] also developed different ray-tracing program, but since programs such as these are difficult to obtain, a new program must be written from scratch to model a LSC.

A Monte Carlo simulation based on ray-tracing model was chosen. It is a statistical model that tracks the progression of photons and applies ray principles [19], such as Snell's law and Beer-Lambert law, as the photons travel in the LSC. Whenever there are different ways for the progression of the photons, random numbers are generated to determine the photons' fate, such as path length, emission angles, etc. The program that was used to handle the Monte Carlo simulation is GoldSim, provided for free by GoldSim Technology Group.

4.1 Assumptions

There are some assumptions that were made to simplify the calculation, and hence the program.

1. The QDs in the solution are assumed to be homogeneously dispersed.

2. The solution is assumed to have the same refractive index as glass.
3. The interface between the solution and glass is assumed to be perfect.
4. At the interface between the glass and air, a photon is either trapped or lost through escape cone, i.e. no partial reflection within the escape cone.
5. All incident light on the LSC is normal to the top plane.
6. All incident light is not reflected off the top surface.

4.2 Simulation algorithm

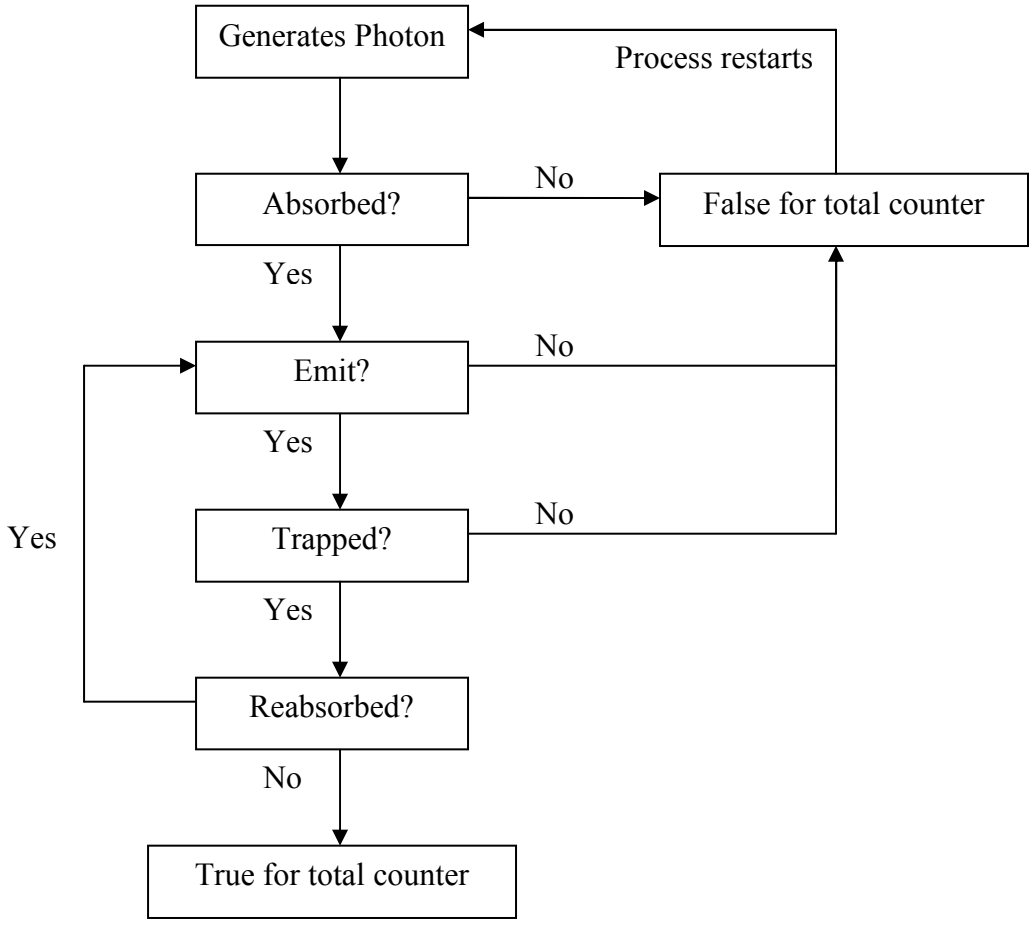

Figure 8: Flow chart of the algorithm in LSC simulation

A flow chat, based on work by Sholin [4], representing the simulation algorithm is presented above. A random number generator is used to assign a wavelength to the photon according to the probability density function associated with the light source (AM1.5 spectrum for sunlight).

The photon then has a chance to be absorbed by the QD. This chance of absorption can be obtained experimentally from a transmission measurement for different wavelengths. From the transmission measurement, the absorption coefficient can be obtained as well. The transmission, T, is given by $T = \frac{I}{I_0} = e^{-\alpha d}$. Solving for α yields

$\alpha = -\frac{\ln(T)}{d}$, where

d is the thickness of the cuvette used in the transmission measurement.

Once the photon is absorbed, it then has a chance to be emitted. The probability of emission is given by the QD's FQY, which can be obtained either experimentally or from sources such as the manufacturer of the QD.

Whenever there is emission, two angles, θ and ϕ, are randomly generated and assigned as the emission angle. The two angles are chosen from uniform distributions because the QD emission is omnidirectional. Only the angle θ is taken into account in the calculation for the trapping. If the angle θ is greater than θ_c, then the photon is trapped inside the LSC.

As mentioned before, each emitted photon has a chance of being reabsorbed before it reaches the collecting edges. If it is not reabsorbed, then the program adds one

to the total counter. If it is reabsorbed, then the program loops back to the emission process for another chance to be re-emitted at two new angles.

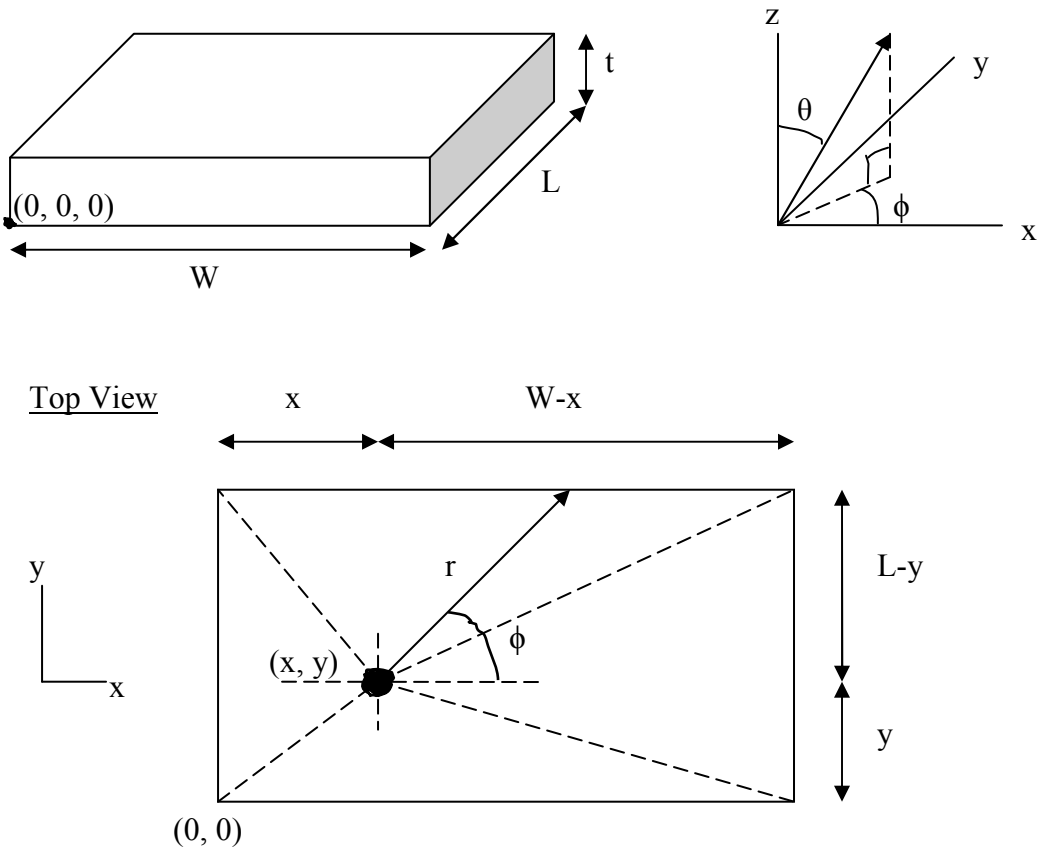

Figure 9: The geometry and top view of the LSC

The process for calculating the reabsorption is slightly more complex than the other processes. Given a random position, (x, y), where the photon is absorbed in the LSC, two random emission angles, θ and ϕ, the width, and the length of the LSC, the total path length needed to reach the collecting edge needs to be found. The idea then is to use the Beer-Lambert equation but it only describes absorption in one dimension. The

first step then is to break down the three dimensional problem into a one dimensional problem.

The top of the LSC is split into four quadrants, indicated by the dashed line touching the corners. It is easier to express the length r through conditional statements because the expression can be found easily.

$$\text{For } 0 \le \phi \le \tan^{-1}\left(\frac{L-y}{W-x}\right) \text{ and } \phi \ge 360° - \tan^{-1}\left(\frac{y}{W-x}\right),\ r = \left|\frac{W-x}{\cos\phi}\right|.$$

$$\text{For } \tan^{-1}\left(\frac{L-y}{W-x}\right) \le \phi \le 180° - \tan^{-1}\left(\frac{L-y}{x}\right),\ r = \left|\frac{L-y}{\sin\phi}\right|.$$

$$\text{For } 180° - \tan^{-1}\left(\frac{L-y}{x}\right) \le \phi \le 270° - \tan^{-1}\left(\frac{x}{y}\right),\ r = \left|\frac{x}{\cos\phi}\right|.$$

$$\text{For } 270° - \tan^{-1}\left(\frac{x}{y}\right) \le \phi \le 360° - \tan^{-1}\left(\frac{y}{W-x}\right),\ r = \left|\frac{y}{\sin\phi}\right|.$$

Side View

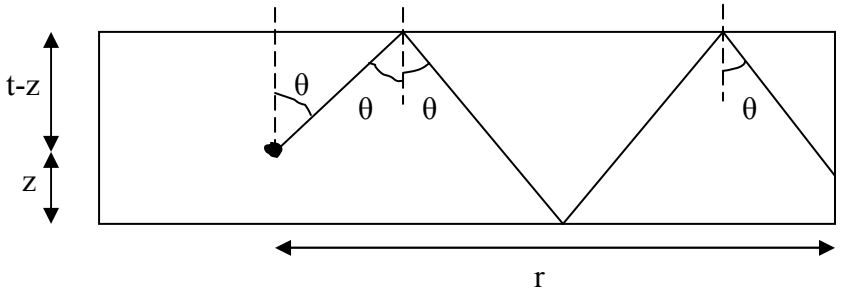

Figure 10: Side view of a slice of r in the LSC

Once r is determined, the total path length to the edge can be found by looking at the side view of a slice of r. The total path length, l_T, is given by

$$l_T = \frac{r}{\sin\theta}.$$

For a given set of six parameters stated earlier, the total path length to the collecting edge is fixed. From the assumption about the partial reflection, θ is always more than 0°, so the case of dividing by zero is not a cause for worry. Interestingly, when it comes to the total path length, the z coordinate and the thickness do not matter in the calculation.

Another parameter that needs to be determined before the reabsorption calculation is the length the photon will travel, denoted as l. This is a randomly assigned number based on a distribution. Starting from Beer-Lambert law, $I = I_0 e^{-\alpha d}$, the probability of photons arriving between two lengths l_2 and l_1 is $Exp(-\alpha l_2) - Exp(-\alpha l_1)$. The probability density is then $\frac{Exp(-\alpha l_2) - Exp(-\alpha l_1)}{l_2 - l_1}$. Taking the limit as Δl approaches zero yields a derivative. The probability density function, P, is then given by

$$P = \left| \lim_{\Delta l \to 0} \frac{Exp(-\alpha l_2) - Exp(-\alpha l_1)}{\Delta l} \right| = \left| \frac{d[Exp(-\alpha l)]}{dl} \right| = \alpha Exp(-\alpha l).$$

Once P is determined, a random l is generated and compared to l_T. If $l \geq l_T$, then the photon reaches the collecting edges. If $l < l_T$, then the photon is reabsorbed. The photon then has a chance to be emitted again taking in account the QD's FQY. If a photon is not re-emitted, then the process starts all over from step one again. When a photon is indeed re-emitted, then the new position where that occurred needs to be determined.

Referring to Figure 11, the length D is given by $D = l\sin(\theta)$. The new coordinate is then

$$(x', y') = (x + D\cos\phi, y + D\sin\phi).$$

Starting with the new position (x', y'), two new angles θ' and ϕ' are randomly chosen assigned, a new total path length to edge l_T' is calculated, and a new l' is assigned from the probability density function, and the whole process, starting from the re-emission, starts over again.

The whole process is repeated N number of times. Since N and the total number of "True" in the counter are known, the optical efficiency of the LSC is then given by

$$\eta_{opt} = \frac{\#\text{ of True}}{\text{N}}.$$

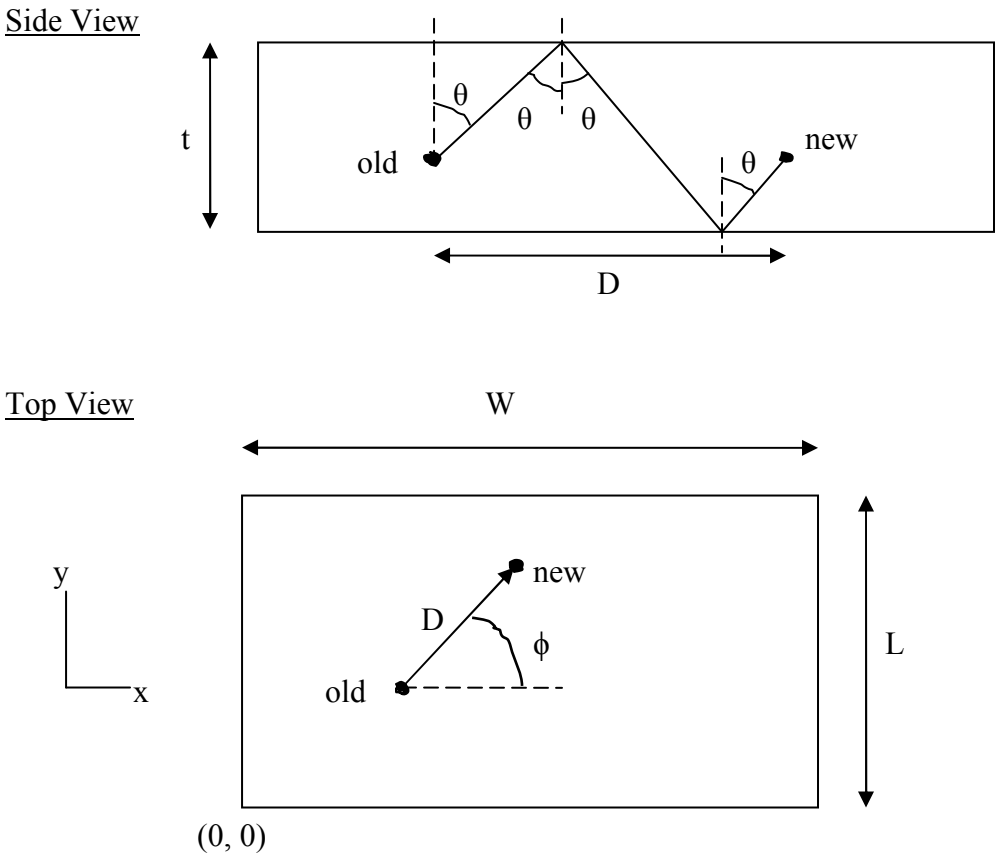

Figure 11: Top and side views for calculating the new position x' and y'

4.3 Simulation results

The data used for the photon generation is the AM1.5 solar spectrum, obtained from National Renewable Energy Laboratory (NREL). The next step is to obtain the transmission data to get the absorption coefficient. A solution of PbSe QD, with concentration of 10 mg/mL in chlorobenzene, was prepared. Using the spectrometer, the transmission spectrum in a 2 mm glass cuvette was obtained.

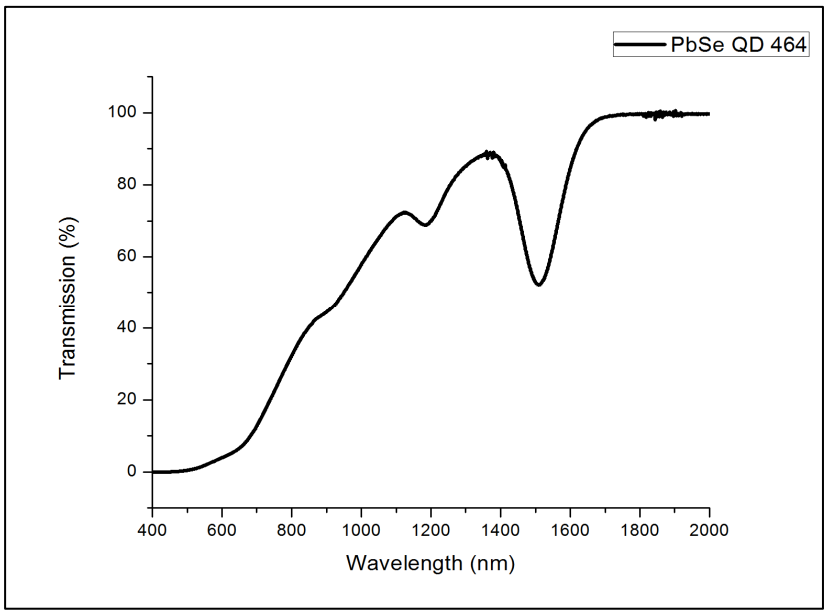

Figure 12: PbSe QD transmission spectrum

For simplification, the refractive index of the solution is assumed to be the same as that of glass, 1.5, therefore θ_c is 41.8°. The FQY of PbSe QD is estimated to be around 0.30. The dimensions of the LSC are assigned to be (50 x 100 x 2) mm. The next thing is to obtain the emission spectrum.

The photoluminescence (PL) test was performed with a 980nm laser as the excitation source. The whole PL setup is illustrated in Figure 13. A chopper spinning at 400 Hz was placed between the laser and sample. The PL of the QD is channeled through a fiber optic cable to a monochrometer and detector, which is connected to a lock-in amplifier. The monochrometer then swept from 900 nm to 2100 nm and the PL signal was logged on the computer. The purpose of the chopper-amplifier system is to improve signal-to-noise ratio.

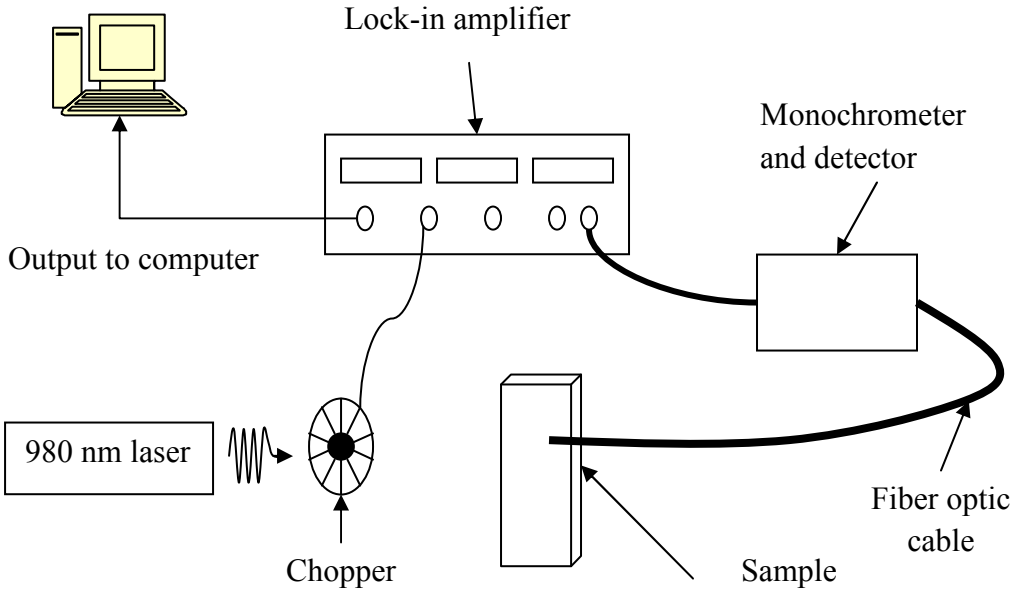

Figure 13: The PL system setup

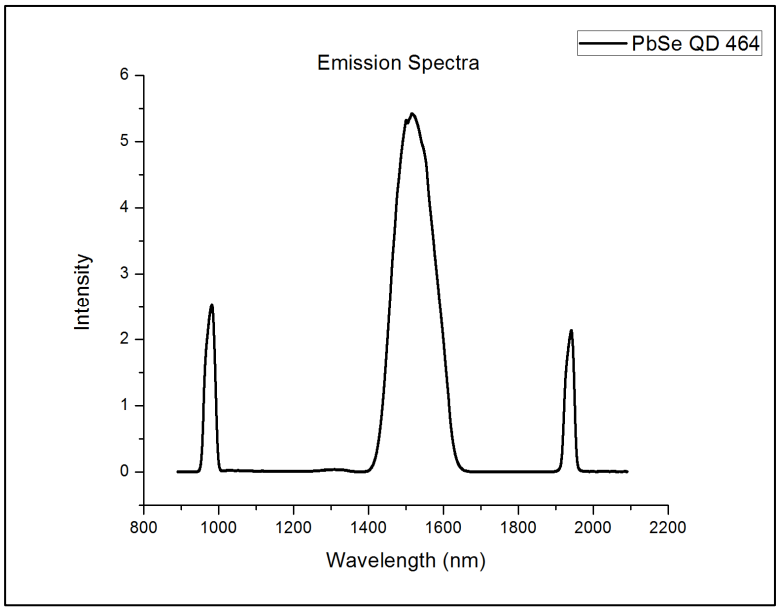

Figure 14: PbSe QD emission spectrum

Shown in Figure 14 is the PbSe QD emission spectrum. The first peak is the signal from the 980 nm laser, used as a reference, the second peak is the PL from the

PbSe QD, and the third peak is the 2nd harmonics of the laser. The emission peak is found to be at 1542 nm. The wavelength dependent absorption coefficient is then obtained from matching the transmission data with the emission data. To reduce computational time, the looping is only carried out to a maximum of 19 times. Once everything is input into the program, the simulation algorithm was repeated for 1 million times, i.e. 1 million photons generate.

The optical efficiency is found to be only 4.47%. This is a very low number which means that the LSC efficiency will be very low as well. Assuming perfect coupling between the LSC and a 20% efficiency solar cell, the LSC efficiency is only 0.89% for the material system described above.

Chapter 5

Additional Experiments

Some brief experiments were conducted to verify a few details about LSC operation.

5.1 Flux/geometric gain experiment

An early investigation into the flux gain was conducted. A thin film of MEH-PPV, ~60 nm thickness was spin coated onto a thin glass substrate. The experimental setup is shown in Figure 15. The amount of exposure is controlled by a slit. A Si detector was placed at the edge to measure the edge output. The signal was recorded as the slit was opened by small increments. Since the slit control the amount of exposure and the sample thickness is constant, this simulates an increasing geometric gain.

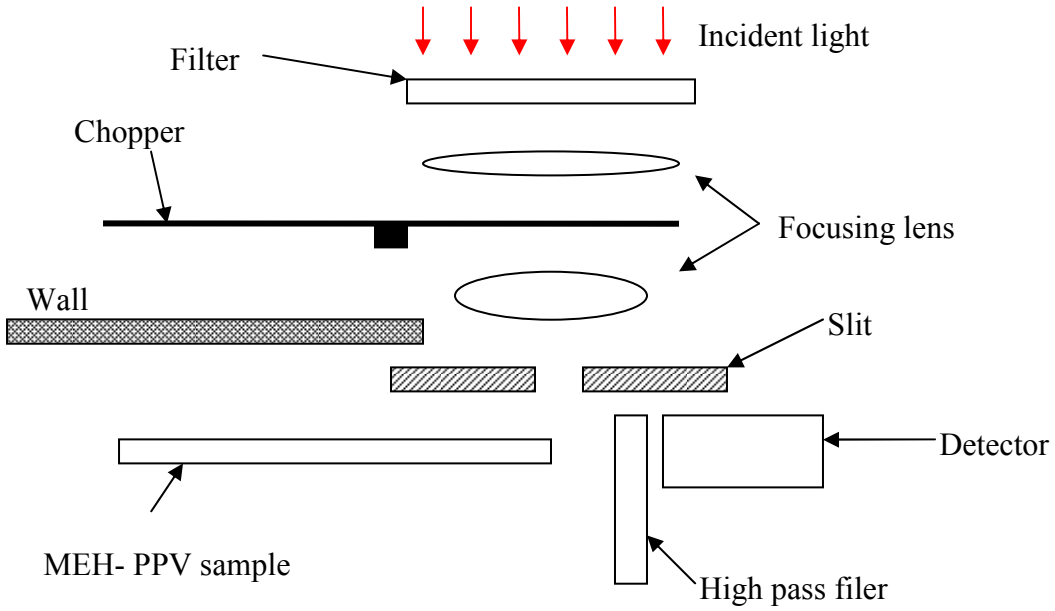

Figure 15: Flux gain experimental setup

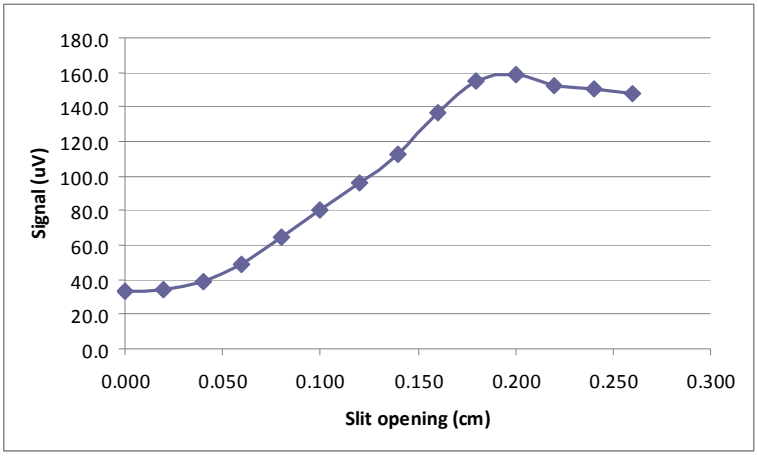

Figure 16: An optimal size

Since the output signal is proportional to the flux gain, the graph indirectly shows the flux gain vs. geometric gain in a LSC. As expected, there is a size at which the signal will start to decrease. A similar experiment with PbSe QD thin film instead of MEH-PPV yields similar results.

5.2 Simple reabsorption loss experiment

A brief experiment shown in Figure 17 was set up. A 2 mm cuvette was filled with PbSe QD. A Ge detector, connected to a voltmeter with a double polished Si was placed at one edge of the cuvette. An 808 nm laser with a spot size of 1 mm diameter was focused near the edge and move away incrementally from the edge. The output signal should decrease as the laser spot is moved away from the edge as the reabsorption loss increases.

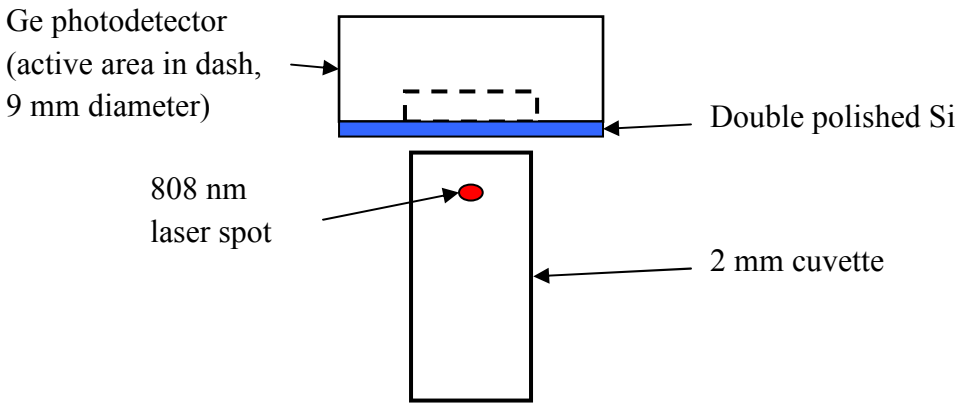

Figure 17: Investigating the reabsorption loss

Table 3: Results from simple reabsorption loss experiment

Distance from edge (mm)	Signal (mV)
2	2.3
6	1.7
10	0.9
13	0.7

A control sample filled with just chlorobenzene was tested as well, with no signal output. As expected, the signal did decrease as the excitation source is moved away.

5.3 Brief experiment on optical efficiency

Lumogen F Red 305 dye (obtained from BASF) was dissolved in toluene to make a solution with concentration of 1.68 mg/mL. A 2 mm cuvette was used as the waveguide and filled with the dye solution. A $GaInP_2$/GaAs/Ge triple junction solar cell from Spectrolab, connected to an ammeter, was then coupled to the cuvette. The light source used was a halogen lamp. The short circuit current of the solar cell was measured under direct illumination and also when it was coupled. The frontal area of the cuvette was measured to be 4.25 cm^2, while the edge area was 0.5 cm^2. Assuming that the solar

cell converts photon approximately the same way for all incoming photon energies larger than the solar cell band gap, i.e. X number of photons will generate a Y number of electron-hole pairs, regardless of wavelength. The optical efficiency can be approximated to be [7],

$$\eta_{opt} = \frac{I_{edge} A_{top}}{I_{top} A_{edge}}, \text{ where}$$

I_{edge} is the short-circuit current measured at the edge, I_{top} is the short-circuit current under direct illumination, A_{top} is the frontal area, and A_{edge} is the edge area. I_{edge} was measured to be 0.19 mA, and I_{top} was measured to be 8.6 mA. Using these values, the optical efficiency was estimated to be around 19%. Assuming perfect coupling between LSC and a solar cell with 20% efficiency, a 19% optical efficiency means a 3.8% LSC efficiency.

Chapter 6

Discussion

Using the simulation model above, the effect of a few selected parameters on the LSC performance will be discussed in this chapter. These parameters are the geometry, FQY, and solution concentration. A feasibility study for the LSC will be discussed as well.

6.1 Geometry

The effect of a square vs. a rectangular LSC was investigated using the simulation described above. Listed in Table 4 are the optical efficiencies of square and rectangular LSCs of 2mm thickness with the same geometric gain.

Table 4: Square vs. rectangular geometry

FQY=0.5

G	Dimension (mm)	Area (mm^2)	Optical Efficiency (%)
1.6667	10 x 20	200	22.74
	13.33 x 13.33	178	22.72
2	10 x 40	400	21.63
	16 x 16	256	21.81
4.1667	20 x 100	2000	16.95
	33.33 x 33.33	1111	16.06
6.25	30 x 150	4500	13.35
	50 x 50	2500	12.36

From Table 4, the optical efficiency does not seem to differ significantly for the same geometric gain. The area required to have a certain geometric gain, however, differ vastly as the geometric gain was increased. The square geometry requires smaller area

for the same geometric gain compared to the rectangular geometry. A smaller area required translates to a cheaper LSC. Therefore a square geometry is definitely better because it will be cheaper to manufacture a LSC of the same geometric gain compared to a rectangular geometry.

6.2 FQY

As mentioned before, a higher FQY should result in higher optical efficiency. Simulations for FQY from 0 to 1 was run for a square LSC with G=6.25.

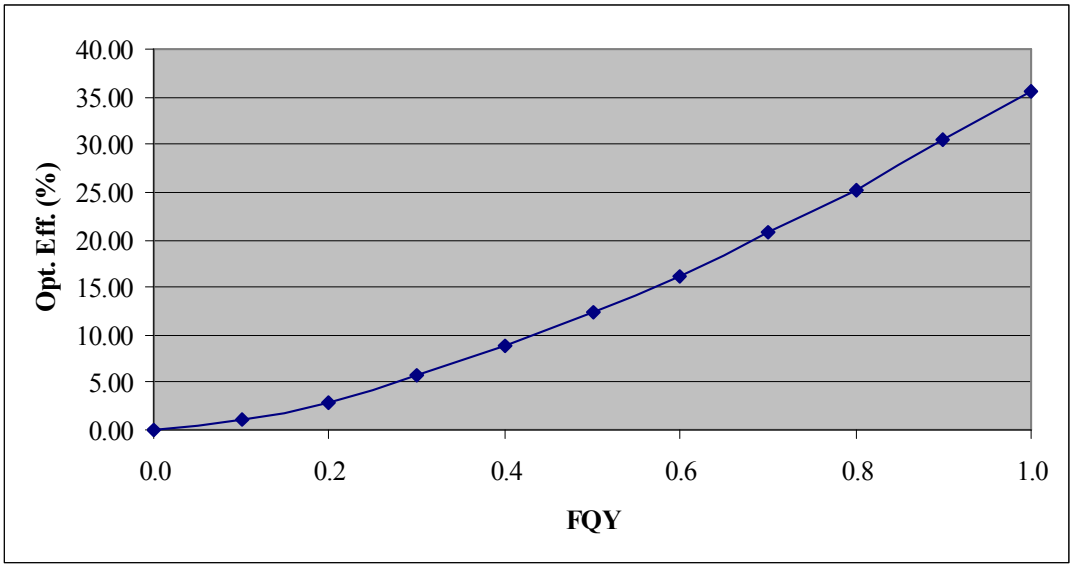

Figure 18: Optical efficiency as a function of FQY

The simulation result showed the trend was just as expected. A FQY=1.0 also gives the theoretical maximum optical efficiency, which is about 35.6% for this particular situation.

6.3 Solution concentration

From the transmission measurement, the transmission data for other solution concentrations were calculated. The absorption coefficient is directly proportional to the solution concentration. If the solution concentration is reduced n times, the new absorption coefficient is given by $\alpha' = \frac{\alpha}{n}$. Therefore the new transmittance, T', is

$$T' = Exp[-\alpha' d] = Exp\left[-\frac{\alpha}{n} d\right] = Exp\left[-\alpha d \frac{1}{n}\right] = T^{\frac{1}{n}}.$$

Once the new wavelength-dependent transmittance is calculated and input into the program, the simulation was run for a square geometry LSC of G=6.25 and FQY=0.3. The results are listed in Table 5.

Table 5: Effect of solution concentration on optical efficiency

FQY=0.3	Solution Concentration	Opt. Eff. (%)
G=6.25	1	5.6
Square	0.5	7.2
	0.25	7.1
	0.1	4.9
	0.01	0.7
	0.001	0.1

The measured solution concentration was normalized to 1, while the rest of the solution concentration data were calculated. As can be seen from Table 5, the solution concentration has an optimal value that maximizes the optical efficiency. From a plot of the optical efficiency vs. solution concentration, the optimal solution concentration was found to be about 0.35, which gives a solution concentration of 3.5 mg/mL.

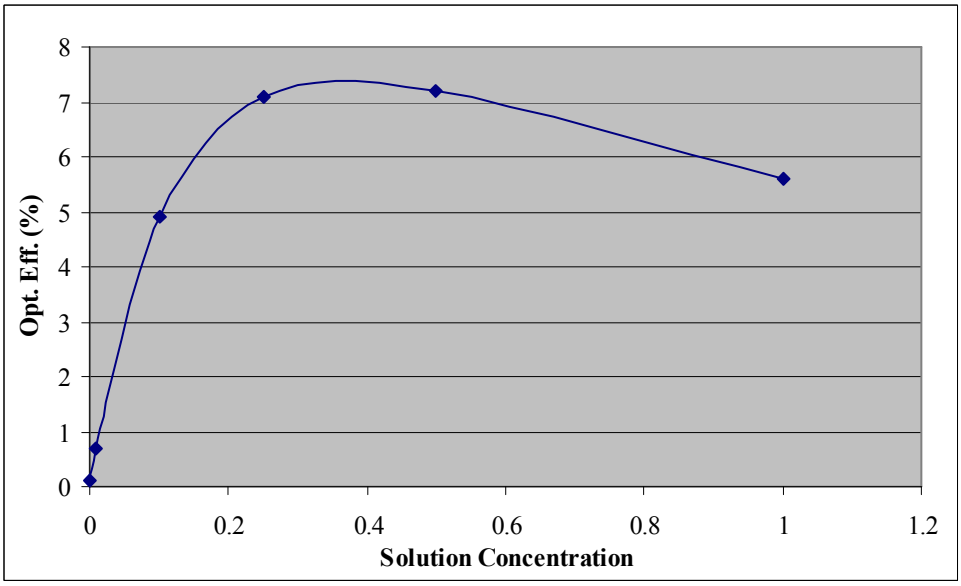

Figure 19: Optical efficiency vs. solution concentration

6.4 Feasibility study

Using the formula for calculating the cost per watt as mentioned before, and using $F = \frac{G\eta_{conc}}{\eta_{PV}}$, the formula becomes

$$\left(\frac{\$}{W}\right)_{LSC} = \frac{\text{collector cost}}{\eta_{conc} P} + \frac{\eta_{PV}}{G\eta_{conc}}\left(\frac{\$}{W}\right)_{\text{solar cell}}.$$

Assuming 1000 W/m^2 intensity, a 50cm x 50cm LSC that cost \$25, coupled to a \$5/W solar cell with 20% efficiency, and a target \$2.50/W LSC, the LSC efficiency needs to be about 4.6% to reach the target cost per watt. Assuming perfect coupling between LSC and the solar cell, the optical efficiency then needs to be at least 23%. This

is a very high number considering the LSC size. Therefore the LSC is still not a feasible idea using the PbSe QDs discussed above.

It is speculated that better manufacturing processes can further narrow the emission spectrum and increase the FQY of QDs. Also with mass production, it is estimated that the collector cost will be driven down significantly. Therefore it is speculated that it could still be feasible for QDs to be used in the LSC design.

6.5 Other factors

As mentioned previously, it was assumed that all the emitted photons within the escape cone were totally lost. Within the escape cone, there is a chance that the emitted photons could be "saved". At the LSC-air interface, there is a chance that the emitted photon will be reflected. There is also the chance of reabsorption within the escape cone. Since the LSC thickness is very small, this reabsorption term is very small as well. While small, including these contributions from reflection and reabsorption can make the model more accurate.

Another factor that could make the model more accurate is incorporating the distinction between actual thickness and effective thickness.

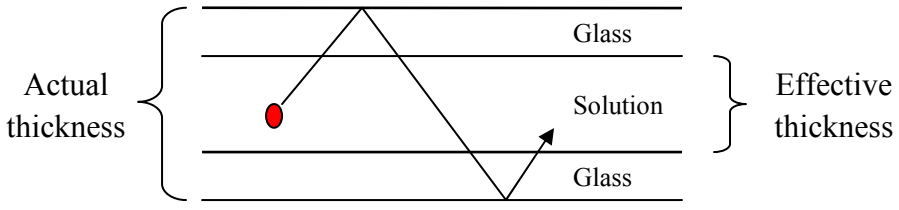

Figure 20: Actual thickness vs. effective thickness

Reabsorption only occurs within the solution. Therefore the path length before the photon is reabsorbed will be increased slightly, and hence the optical efficiency will be increased slightly.

6.6 Solar cell at the edges

Since the LSC thickness is small, the attached solar cell must have small dimension as well. The attached solar cell can be laser-cut from larger solar cells and attached to the edge through a refractive index matching optical coupling [14, 19]. Instead of a regular solar cell that has front and back electrical contacts, one can instead use a solar cell with both electrical contacts at the back, called a point contact solar cell [20-21]. This has the benefit of reduced shading loss due to the absence of the front electrical contact.

Chapter 7

Conclusions

7.1 Accomplished work

A simple Monte Carlo simulation based on ray tracing model has been developed. It was found that a square geometry is more desirable over a rectangular geometry because of the smaller area required to achieve the same effect. Also it was demonstrated that an optimal solution concentration can be found using the simulation. It was found that using the current PbSe QDs material system, it is still not feasible to use the LSC for cost reduction in solar electricity generation.

7.2 Future work

The simulation model can definitely be improved to be more accurate and take into account more factors. Since the addition of mirror will increase the optical efficiency a lot, the first thing that needs to be included is the addition of mirrors or a white scattering layer. Then the effective thickness needs to be taken into account as well. Since the contributions from the reflection of the LSC-air interface and reabsorption within the escape cone are relatively small, those two factors will be taken into account the last.

References

[1] A. Kitai, Luminescent Materials and Applications, John Wiley & Sons, West Sussex, England, 2008

[2] W.H. Weber, J. Lambe, Luminescent greenhouse collector for solar radiation, Appl. Opt. 15 (10) (1976) 2299-2300.

[3] J.A. Levitt, W.H. Weber, Materials for luminescent greenhouse solar collectors, Appl. Opt. 16 (10) (1977) 2684-2689.

[4] D. J. Griffiths, Introduction to Electrodynamics, 3rd ed., Prentice-Hall, New Jersey, 1999.

[5] M. Sidrach de Cardona, et al., Outdoor evaluation of luminescent solar concentrator prototypes, Appl. Opt. 24 (13) (1985) 2028-2032.

[6] B.S. Richards, A. Shalav, R.P. Corkish, A low escape-cone-loss luminescent solar concentrator, in: Proceedings of the 19th European Photovoltaic Solar Energy Conference, Paris, France, 2004, 113-116.

[7] V. Sholin, J.D. Olson, S.A. Carter, Semiconducting polymers and quantum dots in luminescent solar concentrators for solar energy harvesting, J. Appl. Phys. 101 123114 (2007).

[8] S.T. Bailey, et al., Optimized excitation energy transfer in a three-dye luminescent solar concentrator, Sol. Energy Mater. Sol. Cells 91 (2007) 67-75.

[9] B.P. Wittmershaus, et al., Spectral properties of single BODIPY dyes in polystyrene microspheres and in solutions, J. of Fluorescence 11 (2) (2001) 119-128.

[10] J.S. Batchelder, A.H. Zewail, T. Cole, Luminescent solar concentrators 1: Theory of operation and techniques for performance evaluation, Appl. Opt. 18 (18) (1979) 3090-3110.

[11] J.S. Batchelder, A.H. Zewail, T. Cole, Luminescent solar concentrators 2: Experimental and theoretical analysis of their possible efficiencies, Appl. Opt. 20 (21) (1981) 3733-3754.

[12] M.J. Currie, et al., High-efficiency organic solar concentrators for photovoltaics, Science 321 (2008) 226-228.

[13] M.G. Debije, et al., The effect of a scattering layer on the edge output of a luminescent solar concentrator, Sol. Energy Mater. Sol. Cells 93 (2009) 1345-1350.

[14] J.C. Goldschmidt, et al., Increasing the efficiency of fluorescent concentrator systems, Sol. Energy Mater. Sol. Cells 93 (2009) 176-182.

[15] A. A. Earp, et al., Optimisation of a three-colour luminescent solar concentrator daylighting system, Sol. Energy Mater. Sol. Cells 84 (2004) 411-426.

[16] B. C. Rowan, L. R. Wilson, B. S. Richards, Advanced material concepts for luminescent solar concentrators, IEEE J. of Selected Topics in Quantum Electronics 14 (5) (2008) 1312-1322.

[17] M. G. Hyldahl, S. T. Bailey, B. P. Wittmershaus, Photo-stability and performance of CdSe/ZnS quantum dots in luminescent solar concentrators, Solar Energy 83 (2009) 566-573.

[18] S. J. Gallagher, P. C. Eames, B. Norton, Quantum dot solar concentrator behaviour, predicted using a ray trace approach, Int. J. of Ambient Energy 25 (2004) 47-56.

[19] A. R. Burgers, et al., Modelling of luminescent concentrators by ray-tracing, paper presented at the 20th European Photovoltaic Solar Energy Conference and Exhibition, Barcelona, Spain, 6-10 June 2005.

[20] R. M. Swanson, et al., Point-contact silicon solar cells, IEEE Transactions on Electron Devices 31 (5) (1984) 661-664.

[21] R. A. Sinton, et al., Silicon point contact concentrator solar cells, IEEE Electron Device Letters 6 (8) (1985) 405-407.